2009 American Control Conference
Hyatt Regency Riverfront, St. Louis, MO, USA
June 10-12, 2009

Stochastic Modeling of Film Porosity in Thin Film Deposition

Gangshi Hu, Gerassimos Orkoulas and Panagiotis D. Christofides

Abstract— **This work focuses on modeling of film porosity in thin film deposition using stochastic differential equations. A deposition process is modeled via kinetic Monte Carlo (kMC) simulation on a triangular lattice. The microscopic process events involve atom adsorption and migration and the film growth allows for vacancies and overhangs to develop inside the film. Appropriate definitions of film site occupancy ratio (SOR), i.e., fraction of film sites occupied by particles over total number of film sites, and its fluctuation are introduced to describe film porosity. Deterministic and stochastic ordinary differential equation (ODE) models are also derived to describe the time evolution of film SOR and its fluctuation. The coefficients of the ODE models are estimated on the basis of data obtained from the kMC simulator of the deposition process using least-square methods. Simulation results demonstrate the applicability and effectiveness of the proposed film porosity modeling methods in the context of the deposition process under consideration.**

I. Introduction

With the rapid development of the ultra-large scale integration (ULSI) in the semiconductor industry, increased complexity and density of devices on the wafer leads to an increasing demand for improving semiconductor manufacturing process operation and yield. Within this manufacturing environment, thin film microstructure, including thin film surface roughness and amount of internal film defects, has emerged as an important film quality variable which strongly influences the electrical and mechanical properties of microelectronic devices.

Most of the previous research efforts on modeling and control of thin film microstructure have focused on thin film surface roughness, e.g., [13]–[17]. Two fundamental modeling approaches, kinetic Monte Carlo (kMC) methods [3], [6], [7], [20], [21] and stochastic differential equation (SDE) models [4], [5], have been developed to describe the evolution of film microscopic configurations. However, kMC models are not available in closed-form and this limitation precludes the use of kMC models for system-level analysis and the design and implementation of model-based feedback control systems. Therefore, it is desirable to achieve better closed-loop performance by designing feedback controllers on the basis of closed-form process models.

SDEs arise naturally in the modeling of surface morphology of ultra thin films in a variety of material preparation processes [4], [5], [23] since they contain the surface morphology information and account for the stochastic nature of the growth processes. However, the construction of SDE models from kMC simulation data or experimental data is a challenging task. Theoretical foundations on the analysis, parameter optimization, and optimal stochastic control for linear stochastic ordinary differential equation (ODE) systems can be found in the early work by Astrom [1]. More recently, likelihood-based methods for parameter estimation of stochastic ODE models have been developed [2], [11]. These methods determine the model parameters by solving an optimization problem to maximize a likelihood function or a posterior probability density function of a given sequence of measurements of a stochastic process. Recent results [8], [19] employed statistical moments to reformulate the parameter estimation problem into one involving deterministic differential equations.

In the context of modeling of thin film porosity, kMC models have been widely used to model the evolution of porous thin films in many deposition processes, such as the molecular beam epitaxial (MBE) growth of silicon films and copper thin film growth [24], [26]. Both monocrystalline and polycrystalline kMC models have been developed and simulated [12], [25]. Despite recent significant efforts on modeling of surface roughness, a close study of the existing literature indicates the lack of general and practical methods in the area of modeling thin film porosity using SDEs.

Motivated by these considerations, the present work focuses on the development of a systematic methodology for modeling of film porosity in thin film deposition processes using SDEs. Initially, a thin film deposition process which involves atom adsorption and migration is introduced and is modeled using a triangular lattice-based kMC simulator. The film growth model allows porosity, vacancies and overhangs to develop and leads to the deposition of a porous film. Subsequently, appropriate definitions of film site occupancy ratio (SOR) and its fluctuation are introduced to describe film porosity. Then, deterministic and stochastic ODE models are derived that describe the time evolution of film SOR and its fluctuation. The coefficients of the ODE models are estimated on the basis of data obtained from the kMC simulator of the deposition process using least-square methods. Simulation results demonstrate the applicability and effectiveness of the proposed film porosity modeling methods in the context of the deposition process under consideration.

Gangshi Hu and Gerassimos Orkoulas are with the Department of Chemical and Biomolecular Engineering, University of California, Los Angeles, CA 90095 USA.

Panagiotis D. Christofides is with the Department of Chemical and Biomolecular Engineering and the Department of Electrical Engineering, University of California, Los Angeles, CA 90095 USA.

Panagiotis D. Christofides is the corresponding author: Tel: +1(310)794-1015; Fax: +1(310)206-4107; e-mail: pdc@seas.ucla.edu.

Financial support from NSF, CBET-0652131, is gratefully acknowledged.

II. Thin film deposition process description and modeling

This section is associated with the description of the kMC simulation of a thin film deposition process. Two microscopic processes are considered; atom adsorption and surface migration. Vacancies and overhangs are allowed in the kMC model to introduce porosity during the film growth.

A. On-lattice kinetic Monte Carlo model of film growth

The thin film growth process considered in this work includes two microscopic processes: an adsorption process, in which particles are incorporated into the film from the gas phase, and a migration process, in which surface particles move to adjacent sites. A ballistic deposition model is chosen to simulate the evolution of film porosity, which allows vacancies and overhangs to model the microstructural defects in the thin film. Microscopic models with similar rules and structures are reported in simulation works for deposition processes of a variety of materials [12], [24], [25].

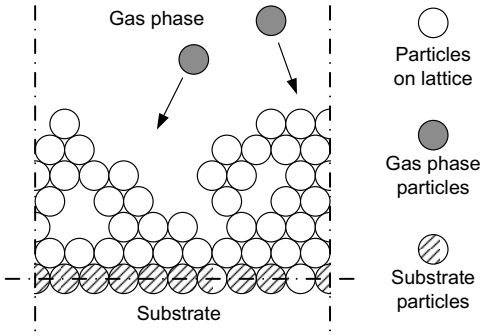

Fig. 1. Thin film growth process on a triangular lattice.

The film growth model used in this work is an on-lattice kMC model in which all particles occupy discrete lattice sites. The on-lattice kMC model is valid for temperatures $T < 0.5T_m$, where T_m is the melting point of the crystal. A triangular lattice is selected to represent the crystalline structure of the film, as shown in Fig.1. All particles are modeled as identical hard disks and the centers of the particles deposited on the film are located on the lattice sites. The diameter of the particles equals the distance between two neighboring sites. The width of the lattice is fixed so that the lattice contains a fixed number of sites in the lateral direction. The new particles are always deposited from the top side of the lattice where the gas phase is located; see Fig.1. Particle deposition results in film growth in the direction normal to the lateral direction. The direction normal to the lateral direction is thus designated as the growth direction. The number of sites in the lateral direction is defined as the lattice size and is denoted by L. The lattice parameter, a, which is defined as the distance between two neighboring sites, determines the lateral extent of the lattice, La.

The number of nearest neighbors of a deposited particle on the thin film ranges from zero to six, the coordination number of the triangular lattice. A particle with six nearest neighbors is associated with an interior particle that is fully surrounded by other particles and cannot migrate. A particle with one to five nearest neighbors is possible to diffuse to an unoccupied neighboring site with a probability that depends on its local environment. In the simulation, a bottom layer in the lattice is initially set to be fully packed and fixed, as shown in Fig.1. There are no vacancies in this layer and the particles in this layer cannot migrate. This layer acts as the substrate for the deposition and is not counted in the computation of the number of the deposited particles, i.e., this fixed layer does not influence the film porosity (see section III below).

Two types of microscopic processes (Monte Carlo events) are considered, an adsorption process and a migration process. These Monte Carlo events are assumed to be Poisson processes. All events occur randomly with probabilities proportional to their respective rates. The events are executed instantaneously upon selection and the state of the lattice remains unchanged between two consecutive events.

B. Adsorption process

In an adsorption process, an incident particle comes in contact with the film and is incorporated onto the film. The microscopic adsorption rate, W, which is in units of layers per unit time, depends on the gas phase concentration. The layers in the unit of adsorption rate are densely packed layers, which contain L particles. With this definition, W is independent of L. In this work, the microscopic adsorption rate, W, is treated as a process parameter. For the entire deposition process, the macroscopic adsorption rate in terms of incident particles per unit time, which is denoted as r_a, is related to W as follows:

$$r_a = LW \tag{1}$$

The incident particles are initially placed at random positions above the film lattice and move toward the lattice in random directions. The initial particle position, x_0, which is the center of an incident particle, is uniformly distributed in the continuous domain, $(0, La)$. The incident angle, θ, is defined as the angle between the incident direction and the direction normal to the film, with a positive value assigned to the down-right incident direction and a negative value assigned to the down-left incident direction. Probability distribution functions of the incident angle may vary from a Dirac-Delta function to a cosine function, for different deposition processes. In this work, the probability distribution of the angle of incidence is chosen to be uniform in the interval $(-0.5\pi, 0.5\pi)$.

The procedure of an adsorption process is illustrated in Fig.2. After the initial position and incident angle are determined, the incident particle, A, travels along a straight line towards the film until contacting the first particle, B, on the film. Upon contact, particle A stops and sticks to particle B at the contacting position; see Fig.2. Then, particle A moves (relaxes) to the nearest vacant site, C, among the neighboring sites of particle B. Instantaneous particle surface relaxation is conducted since site C has only one neighboring particle and is considered unstable in the triangular lattice,

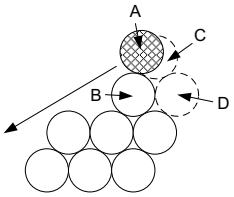

Fig. 2. Schematic of the adsorption event with surface relaxation. In this event, particle A is the incident particle, particle B is the surface particle that is first hit by particle A, site C is the nearest vacant site to particle A among the sites that neighbor particle B, and site D is a stable site where particle A relaxes.

as shown in Fig.2. When a particle is subject to particle surface relaxation, the particle moves to its most stable neighboring vacant site, which is defined as the site with the most nearest neighbors. In the case of multiple neighboring vacant sites with the same number of nearest neighbors, a random one is chosen from these sites with equal probability as the objective of the particle surface relaxation process. Note that particle surface relaxation is considered as part of the deposition event, and thus, it does not contribute to the process simulation time. There is also only one relaxation event per incident particle.

C. Migration process

In a migration process, a particle overcomes the energy barrier of the site and jumps to its vacant neighboring site. The migration rate (probability) of a particle follows an Arrhenius-type law with a pre-calculated activation energy barrier that depends on the local environment of the particle, i.e., the number of the nearest neighbors of the particle chosen for a migration event. The migration rate of the ith particle is calculated as follows:

$$r_{m,i} = \nu_0 \exp\left(-\frac{n_i E_0}{k_B T}\right) \tag{2}$$

where ν_0 denotes the pre-exponential factor, n_i is the number of the nearest neighbors of the ith particle and can take the values of 2, 3, 4 and 5 ($r_{m,i}$ is zero when $n_i = 6$ since this particle is fully surrounded by other particles and cannot migrate), E_0 is the contribution to the activation energy barrier from each nearest neighbor, k_B is the Boltzmann's constant and T is the substrate temperature of the thin film. Since the film is thin, the temperature is assumed to be uniform throughout the film and is treated as a time-varying but spatially-invariant process parameter. In this work, the factor and energy barrier contribution in Eq.2 take the following values $\nu_0 = 10^{13}\text{s}^{-1}$ and $E_0 = 0.6$ eV, which are appropriate for a silicon film [10].

When a particle is subject to migration, it can jump to either of its vacant neighboring sites with equal probability, unless the vacant neighboring site has no nearest neighbors, i.e., the surface particle cannot jump off the film and it can only migrate on the surface.

D. Simulation algorithm

After the rates of surface micro-processes are determined, kMC simulations can be carried out using the continuous-time Monte Carlo method [22] due to the computational efficiency. To simulate the process with limited-size lattice and reduce the boundary effects, periodic boundary conditions (PBCs) are applied to the kMC model of the deposition process. With the assumption that all microscopic processes are Poisson processes, the time increment upon the execution of a successful event is computed based on the total rates of all the micro-processes, which can be listed and calculated from the current state of the lattice. To further improve the computational efficiency, a grouping algorithm is also used in the selection of the particle that is subject to migration [18]. In the grouping algorithm, the events are pre-grouped to improve the execution speed. In this work, the layer of the film emerges as a natural grouping criterion, i.e., all particles in the same layer are considered to be part of one group.

III. Open-loop simulations

In this section, simulations of the kMC model of a silicon thin film growth process using the methodology described in the previous section are presented with the process parameters being kept constant (i.e., open-loop simulation). Appropriate definitions of film site occupancy ratio are also introduced to describe the film porosity and its fluctuation.

A. Definition of film site occupancy ratio

Since film porosity is the main objective of modeling and control design of this work, a new variable, film site occupancy ratio (SOR), is introduced to represent the extent of the porosity inside the thin film as follows:

$$\rho = \frac{N}{LH} \tag{3}$$

where ρ denotes the film SOR, N is the total number of deposited particles on the lattice, L is the lattice size (i.e., number of sites in one layer), and H denotes the number of deposited layers. Note that the deposited layers are the layers that contain deposited particles and do not include the initial substrate layer. The concept of packing density, which represents the occupancy ratio of space for a specific packing method, is not the same as the film SOR defined in Eq.3, and thus, it cannot be used to characterize the evolution of film porosity.

Fig.3 gives an example showing how film SOR is defined. Since each layer contains L sites, the total number of sites in the film is LH. Film SOR is the ratio between the number of deposited particles, N, and the total number of sites, LH. With this definition, film SOR ranges from 0 to 1. Specifically, $\rho = 1$ denotes a film whose sites are fully occupied and has a flat surface. At the beginning of the deposition process when there are no particles deposited on the lattice and only the substrate layer is present, N and H are both zeros and the ratio $N/(LH)$ is not defined. In this case, a zero value is assigned to the film SOR at this state. As a consequence, the evolution profiles of the film SOR in this work always start from zero.

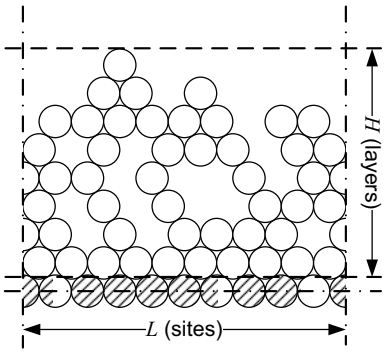

Fig. 3. Illustration of the definition of film SOR of Eq.3.

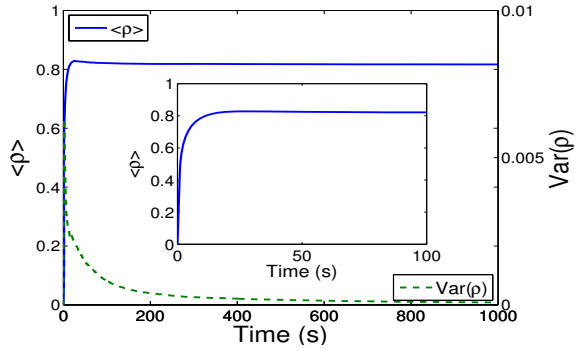

Fig. 4. Mean value (solid lines) and variance (dashed line) of the complete film SOR versus time for a 1000 s open-loop deposition process with substrate temperature $T = 600$ K and deposition rate $W = 1$ layer/s.

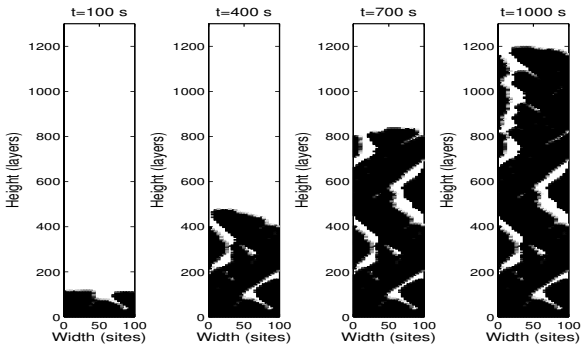

Fig. 5. Snapshots of the film microstructure at $t = 100$ s, 400 s, 700 s and 1000 s of the open-loop deposition process with substrate temperature $T = 600$ K and deposition rate $W = 1$ layer/s.

Due to the stochastic nature of kMC models of thin film growth processes, the film SOR, ρ, fluctuates about a mean value, $\langle\rho\rangle$, at all times. A quantitative measure of the SOR fluctuations is provided by the variance of the film SOR as follows:

$$\mathrm{Var}(\rho) = \left\langle (\rho - \langle\rho\rangle)^2 \right\rangle \tag{4}$$

where $\langle\cdot\rangle$ denotes the average (mean) value.

B. Film site occupancy ratio evolution profiles

In this subsection, the thin film deposition process is simulated according to the algorithm described in section II. The evolution of film SOR defined in Eq.3 and its variance are computed from Eqs.3 and 4, respectively. The lattice size L is equal to 100 throughout this work. The choice of lattice size is determined from a balance between statistical accuracy and reasonable requirements for computing power. 1000 independent simulation runs are carried out to obtain the expected value and the variance of the film SOR. The simulation time is 1000 s. All simulations start with an identical flat initial condition, i.e., only a substrate layer is present on the lattice without any deposited particles. Fig.4 shows the evolution profiles of the film SOR and its variance during the deposition process for the following process parameters: $T = 600$ K and $W = 1$ layer/s. In Fig.4, the film SOR is initially 0 and as particles begin to deposit on the film, the film SOR increases with respect to time and quickly reaches a steady-state value. Snapshots of the thin film microstructure at different times, $t = 100$ s, 400 s, 700 s and 1000 s, of the open-loop simulation are shown in Fig.5.

In Fig.4, the evolution profile of the variance starts at zero and jumps to a peak, after which the variance decays with respect to time. The variance is used to represent the extent of fluctuation of the film SOR at a given time. Since all simulations start at the same initial condition, the initial variance is zero (by convention) at time $t = 0$. As particles begin to deposit on the film, the variance of the film SOR, $\mathrm{Var}(\rho)$, increases at short times and it subsequently decreases to zero at large times. Note that the film SOR is a cumulative property since it accounts for all the deposited layers and particles on the film. Thus, at large times, SOR fluctuations decrease as more layers are included into the film. It is evident from Fig.4 that the SOR variance decays and approaches zero at large times. Thus, the film SOR of Eq.3 and its variance of Eq.4 are not suitable variables for the purposes of modeling and control of film porosity fluctuations. Another variable must be introduced to represent the fluctuation of the film porosity for modeling and control purposes.

C. Partial film site occupancy ratio

In this subsection, a new concept of film SOR is introduced, termed partial film SOR, which is the film SOR calculated by accounting only for the top H_p layers of the film. Mathematically, the partial film SOR is defined as follows:

$$\rho_p = \frac{N_p}{LH_p} \tag{5}$$

where ρ_p denotes the partial film SOR and N_p denotes the number of particles in the top H_p layers and H_p denotes the number of top layers of the film included in the computation of the partial film SOR. The definition of the partial film SOR is shown schematically in Fig.6. To calculate the partial film SOR of Eq.5, the number of top H_p layers must first be determined. As shown in Fig.6, the top H_p layers start from the top layer of the lattice and include the (H_p-1) layers below the top layer. The number of particles in the top H_p layers is denoted by N_p. The partial film SOR, ρ_p, is then calculated as the ratio between N_p and the total number of

sites in the top H_p layers, LH_p. Similar to ρ, ρ_p is ranging from 0 to 1. $\rho_p = 1$ denotes fully occupied top H_p layers.

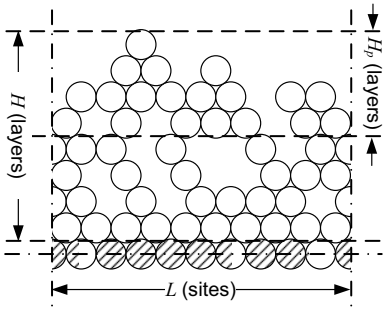

Fig. 6. Illustration of the definition of partial film SOR of Eq.5.

The choice of H_p affects the value of the partial film SOR, ρ_p, and furthermore, it results in different modeling results. Specifically, the partial film SOR cannot be correctly calculated without the existence of H_p layers in the film. This problem is bypassed by assuming the existence of H_p fully-packed substrate layers in the film before the deposition process begins. These substrate layers are used in the calculation of ρ_p when $H < H_p$; see, for example, Fig.7 for the construction of the substrate layers. This assumption does not affect the deposition process since the particles in the substrate layers neither migrate nor affect the adsorption or migration processes of the deposited particles. Therefore, at the beginning of deposition, the partial film SOR starts from unity since all H_p layers are substrate layers and are fully occupied. There also exist alternative choices of H_p at the beginning of deposition, e.g., equating H_p with H and hence having $\rho_p = \rho$ when $H < H_p$. Different choices of H_p affect the computation of ρ_p at the initial stages and result in different initial values. However, the main dynamics of the partial film SOR remains unchanged, especially at large times.

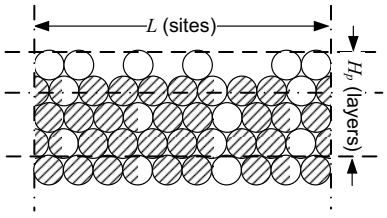

Fig. 7. Illustration of the substrate layers used in the definition of partial film SOR at the initial stage. Underneath the deposited particles (white particles), all layers are filled with particles (shadowed particles) and are used for the calculation of the partial film SOR until H_p film layers have been deposited.

Although complete film SOR and partial film SOR are defined similarly, they are different variables, which are used to describe different aspects of the film. The most notable difference is the denominator of the fractions. In the complete film SOR, the denominator of the ratio is the number of the sites in the entire deposited film, and thus, it increases with respect to time, due to the deposition of new particles. This cumulative property of the complete film SOR averages the fluctuations of the porosity from different layers of the film and results in the decay of the variance of the complete film SOR to zero with respect to time. For the partial film SOR, on the contrary, the denominator of the ratio is fixed at LH_p, and thus, ρ_p only accounts for the porosity of the newly deposited H_p layers of the film. Another difference lies in the mechanism of the deposition process. Due to particle migration, particles in the film interior have a higher probability of achieving closed-packed configurations than particles in the top layers. However, newly deposited particles in the top layers have not experienced enough migration events and are more active for migrating. For the above reasons, the fluctuation of ρ_p does not decay with respect to time and is much larger than the fluctuation of ρ at large times. Thus, the variance of ρ_p is selected to represent the porosity fluctuations and is used for modeling and control design. The partial film SOR variance, $\mathrm{Var}(\rho_p)$, is computed by the following expression

$$\mathrm{Var}(\rho_p) = \left\langle (\rho_p - \langle \rho_p \rangle)^2 \right\rangle. \tag{6}$$

The evolution profiles of the expected partial film SOR and the variance of partial film SOR are shown in Figs.8 for the same process parameters as in Fig.4. The top 100 layers are chosen in the calculation of the partial film SOR, i.e., $H_p = 100$ in Eq.5. The choice of H_p depends on the process requirements. Too few layers result in dramatic fluctuations of the partial film SOR. For a deposition process of about 1000 deposited layers, it is found through extensive simulation tests that 100 top layers constitute a suitable choice for modeling and control design.

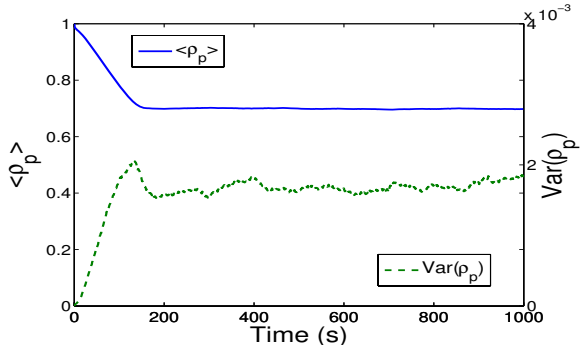

Fig. 8. Mean value (solid line) and variance (dashed line) of the partial film SOR versus time for a 1000 s open-loop deposition process with substrate temperature $T = 600$ K and deposition rate $W = 1$ layer/s.

As shown in Fig.8, the mean partial film SOR, $\langle \rho_p \rangle$, starts from 1 as a result from the use of the initial substrate layer. Then, $\langle \rho_p \rangle$ decreases with respect to time and reaches a steady-state value at large times. Comparing to the expected film SOR in Fig.4, the expected partial film SOR is smaller at steady state, since the top layers of the film are newly formed and are more active for particle migration than the bulk layers, which are already deposited for a longer time and are stabilized.

The evolution profile of the variance of partial film SOR, $\mathrm{Var}(\rho_p)$, is different from the one of the complete film SOR, $\mathrm{Var}(\rho)$, which decays to zero at large times. Similarly to the evolution of $\mathrm{Var}(\rho)$, $\mathrm{Var}(\rho_p)$ starts from zero due to an identical deterministic initial condition applied to all simulations. However, $\mathrm{Var}(\rho_p)$ does not decay to zero with respect to time, but reaches a steady-state non-zero value. Therefore, the variance of partial film SOR is chosen as the representation of the run-to-run fluctuation of film porosity.

IV. Construction of ODE models for complete and partial film site occupancy ratio

For modeling and control purposes, dynamic models are required that describe the evolution of film porosity in terms of complete and partial film SOR. In this section, deterministic and stochastic linear ODE models are derived to describe the evolution of film SOR. The derivation of these ODE models and the computation of their parameters is done on the basis of data obtained from the kMC model of the deposition process.

A. Deterministic dynamic model of complete film site occupancy ratio

From the open-loop simulation results, the dynamics of the expected value of the complete film SOR evolution can be approximately described by a first-order ODE model. Therefore, a linear first-order deterministic ODE is chosen to describe the dynamics of the complete film SOR as follows:

$$\tau \frac{d\langle \rho(t)\rangle}{dt} = \rho^{ss} - \langle \rho(t)\rangle \tag{7}$$

where t is the time, τ is the time constant and ρ^{ss} is the steady-state value of the complete film SOR. The deterministic ODE system of Eq.7 is subject to the following initial condition:

$$\langle \rho(t_0)\rangle = \rho_0 \tag{8}$$

where t_0 is the initial time and ρ_0 is the initial value of the complete film SOR. Note that ρ_0 is a deterministic variable, since ρ_0 refers to the expected value of the complete film SOR at $t = t_0$. From Eqs.7 and 8, it follows that

$$\langle \rho(t)\rangle = \rho^{ss} + (\rho_0 - \rho^{ss})\, e^{-(t-t_0)/\tau}. \tag{9}$$

B. Stochastic dynamic model of partial film site occupancy ratio

To capture the variance of the partial film SOR, a stochastic model must be used. For simplicity, a linear stochastic ODE is used to model the dynamics of the partial film SOR. Similarly to the deterministic ODE model for the expected complete film SOR of Eq.7, a first-order stochastic ODE is chosen for the computation of the partial film SOR as follows:

$$\tau_p \frac{d\rho_p(t)}{dt} = \rho_p^{ss} - \rho_p(t) + \xi_p(t) \tag{10}$$

where ρ_p^{ss} and τ_p are the two model parameters which denote the steady-state value of the partial film SOR and the time constant, respectively, and $\xi_p(t)$ is a Gaussian white noise with the following expressions for its mean and covariance:

$$\begin{aligned} \langle \xi_p(t)\rangle &= 0 \\ \langle \xi_p(t)\xi_p(t')\rangle &= \sigma_p^2 \delta(t-t') \end{aligned} \tag{11}$$

where σ_p is a parameter which measures the intensity of the Gaussian white noise and $\delta(\cdot)$ denotes the standard Dirac delta function. The model parameters ρ_p^{ss}, τ_p and σ_p are functions of the substrate temperature. We note that $\xi_p(t)$ is taken to be a Gaussian white noise because the values of ρ_p obtained from $10,000$ independent kMC simulations of the deposition process at large times are in closed accordance with a Gaussian distribution law: see Fig.9 for the histogram of the partial film SOR at $t = 1000$ s.

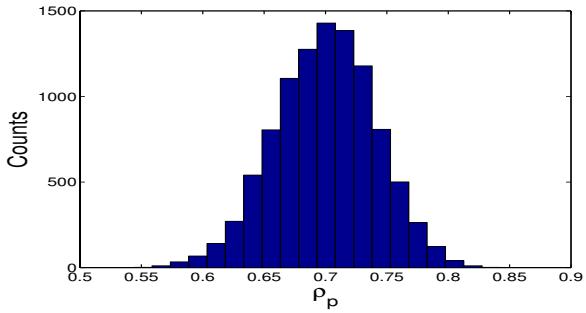

Fig. 9. Histogram from $10,000$ simulation runs of the partial film SOR at the end ($t = 1000$ s) of the open-loop deposition process with substrate temperature $T = 600$ K and deposition rate $W = 1$ layer/s.

The stochastic ODE system of Eq.10 is subject to the following initial condition:

$$\rho_p(t_0) = \rho_{p0} \tag{12}$$

where ρ_{p0} is the initial value of the partial film SOR. Note that ρ_{p0} is a random number, which follows a Gaussian distribution.

The following analytical solution of Eq.10 can be obtained from a direct computation as follows:

$$\rho_p(t) = \rho_p^{ss} + \left(\rho_{s0} - \rho_p^{ss}\right) e^{-(t-t_0)/\tau_p} + \int_{t_0}^{t} e^{-(s-t_0)/\tau_p} \xi_s ds. \tag{13}$$

In Eq.13, $\rho_p(t)$ is a random process, the expected value of which, $\langle \rho_p(t)\rangle$, can be obtained as follows:

$$\langle \rho_p(t)\rangle = \rho_p^{ss} + \left(\langle \rho_{s0}\rangle - \rho_p^{ss}\right) e^{-(t-t_0)/\tau_p}. \tag{14}$$

The analytical solution of $\mathrm{Var}(\rho_p)$ can be obtained from the solution of Eq.13 using the following result [1]:

Result 1: If (1) $f(x)$ is a deterministic function, (2) $\eta(x)$ is a random process with $\langle \eta(x)\rangle = 0$ and covariance $\langle \eta(x)\eta(x')\rangle = \sigma^2 \delta(x-x')$, and (3) $\varepsilon = \int_a^b f(x)\eta(x)dx$, then ε is a real random variable with $\langle \varepsilon\rangle = 0$ and variance $\langle \varepsilon^2\rangle = \sigma^2 \int_a^b f^2(x)dx$.

Using Result 1, the variance of the partial film SOR, $\mathrm{Var}(\rho_p)$, can be obtained from the analytical solution of Eq.13 as follows:

$$\mathrm{Var}(\rho_p(t)) = \frac{\tau_p \sigma_p^2}{2} + \left(\mathrm{Var}(\rho_{p0}) - \frac{\tau_p \sigma_p^2}{2}\right) e^{-2(t-t_0)/\tau_p} \tag{15}$$

where $\mathrm{Var}(\rho_{p0})$ is the variance of the partial film SOR at time $t = 0$, which is calculated as follows:

$$\mathrm{Var}(\rho_{p0}) = \left\langle (\rho_{p0} - \langle \rho_{p0} \rangle)^2 \right\rangle. \quad (16)$$

A new model parameter, Var_p^{ss}, is introduced to simplify the solution of $\mathrm{Var}(\rho_p)$ in Eq.15 as follows:

$$\mathrm{Var}_p^{ss} = \frac{\tau_p \sigma_p^2}{2} \quad (17)$$

where Var_p^{ss} stands for the steady-state value of the variance of the partial film SOR. With the introduction of this new model parameter, the solution of the variance of the partial film SOR, $\mathrm{Var}(\rho_p)$, can be rewritten in the following form:

$$\mathrm{Var}(\rho_p(t)) = \mathrm{Var}_p^{ss} + \left(\mathrm{Var}(\rho_{p0}) - \mathrm{Var}_p^{ss}\right) e^{-2(t-t_0)/\tau_p}. \quad (18)$$

C. Parameter estimation

Since the ODE models of Eqs.7 and 10 are linear, the five parameters, ρ^{ss}, τ, ρ_p^{ss}, τ_p and Var_p^{ss}, can be estimated from the solutions of Eqs.9 and 14. Specifically, the parameters ρ_p^{ss} and τ_p are estimated using Eq.9 and the parameters ρ_p^{ss}, τ_p and Var_p^{ss} are estimated using Eq.14, solving two separate least square problems. Specifically, the two least-square problems can be solved independently to obtain the first four model parameters. The steady-state variance, Var_p^{ss}, is obtained from the steady-state values of the variance evolution profiles at large times.

The parameters ρ^{ss} and τ are estimated by minimizing the sum of the squared difference between the evolution profiles from the ODE model prediction and the kMC simulation at different time instants as follows:

$$\min_{\rho^{ss},\tau} \sum_{i=1}^{m} \left[\langle \rho(t_i) \rangle - \left(\rho^{ss} + (\rho_0 - \rho^{ss}) e^{-(t-t_0)/\tau} \right) \right]^2 \quad (19)$$

where m is the number of the data pairs, $(t_i, \langle \rho(t_i) \rangle)$, from the kMC simulations. Similarly, ρ_p^{ss} and τ_p can be obtained by solving the following least-square optimization problem expressed in terms of the expected partial film SOR:

$$\min_{\rho_p^{ss},\tau_p} \sum_{i=1}^{m} \left[\langle \rho_p(t_i) \rangle - \left(\rho_p^{ss} + (\rho_{p0} - \rho_p^{ss}) e^{-2(t-t_0)/\tau_p} \right) \right]^2. \quad (20)$$

The data used for the parameter estimation are obtained from the open-loop kMC simulation of the thin film growth process. These data can be obtained from off-line measurements, but real-time estimates of film porosity is also possible by using the on-line measurement data, such as surface height profiles. The process parameters are fixed during each open-loop simulation so that the dependence of the model parameters on the process parameters can be obtained for fixed operation conditions. The complete film SOR and the partial film SOR are calculated on the basis of the deposited film at specific time instants.

The above parameter estimation process is applied to the open-loop simulation results. First, the open-loop evolution profiles of the complete film SOR and of the partial film SOR are obtained from 1000 independent kMC simulation runs with substrate temperature $T = 600$ K and deposition rate $W = 1$ layer/s. Subsequently, the deterministic and stochastic ODE models of Eqs.7 and 10 are compared with the open-loop kMC simulation data to compute the model parameters using least square methods. Figs.10 and 11 show the open-loop profiles and the predicted profiles of $\langle \rho \rangle$, $\langle \rho_p \rangle$ and $\mathrm{Var}(\rho_p)$ from the ODE models with the estimated parameters as follows:

$$\begin{aligned} &\rho^{ss} = 0.8178, \quad \tau = 1.6564 \text{ s} \\ &\rho_p^{ss} = 0.6957, \quad \tau_p = 77.27 \text{ s}, \quad \mathrm{Var}_p^{ss} = 1.6937 \times 10^{-3}. \end{aligned} \quad (21)$$

The predictions from the ODE models are very close to the open-loop kMC simulation profiles, which indicates that the dynamics of the film SOR can be adequately described by first-order ODEs. There is, however, some mismatch of the predicted ODE-based profiles from the kMC data, especially for the expected value of the complete film SOR. This is because the dynamics of the complete film SOR depend on the total height of the film. A film at initial stages is very thin and the complete film SOR changes significantly as more layers are deposited, while a film at large times is much thicker and the complete film SOR is relatively insensitive to the newly deposited layers. Since a first-order ODE model is used to capture the dynamics of the complete film SOR, the time constant, τ, is chosen to strike a balance between the initial and final stages of the film growth. Therefore, the predictions from the ODE model cannot match the open-loop profiles, obtained from the kMC models, perfectly at all times. Overall, the computed first-order ODE models approximate well the dynamics of the film SOR and its fluctuation, and thus, they can be used for the purpose of feedback control design.

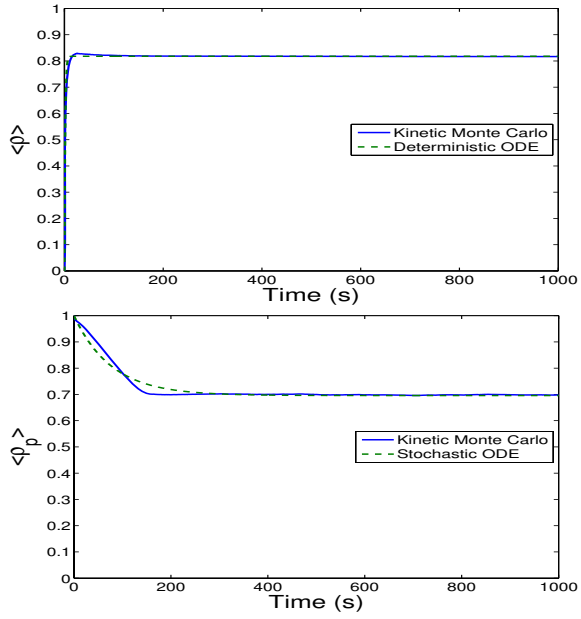

Fig. 10. Expected value of the complete film SOR (Top) and the partial film SOR (bottom) with respect to time for a 1000 s open-loop deposition process (solid line) and predictions from the deterministic/stochastic ODE models with estimated parameters (dashed line); $T = 600$ K, $W = 1$ layer/s.

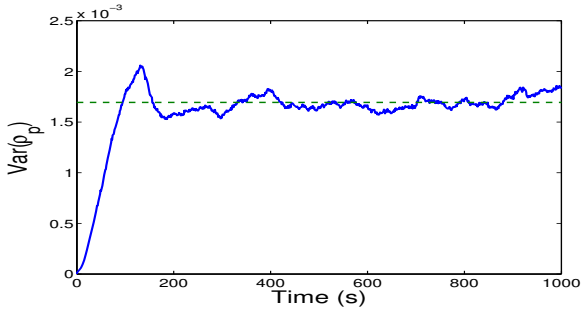

Fig. 11. Variance of the partial film SOR with respect to time for a 1000 s open-loop deposition process (solid line) and the estimated steady-state level (dashed line); $T = 600$ K, $W = 1$ layer/s.

The dependence of model parameters on the process variables, i.e., the substrate temperature and the adsorption rate, can be obtained by repeating the estimation process at a variety of operating conditions. Such dependence can be used in the predictive control design which regulates the film porosity at a desired level and minimizes the porosity fluctuations [9].

Finally, the lattice size dependence of the steady-state value of complete film SOR is shown in Fig.12. It can be clearly seen that the film SOR depends on the lattice size. To achieve near lattice-size independence, a very large lattice size is required and cannot be simulated using the available amount of computing power. The purpose of the proposed modeling method is to identify the film SOR models from the output of the given deposition process, which can be from either a kMC simulator or experimental deposition process data. Note that the applicability of the proposed modeling method is not limited to any specific lattice size. In this work, a lattice size of 100 captures the film SOR dynamics and allows obtaining sufficient statistical accuracy in terms of computing expected values and variances of film SORs.

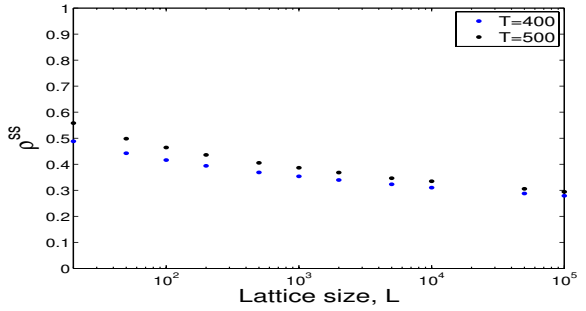

Fig. 12. Dependence of steady-state values of film SOR, ρ^{ss}, on the lattice size for different temperature.

REFERENCES

[1] K. J. Åström. *Introduction to Stochastic Control Theory*. Academic Press, New York, 1970.

[2] T. Bohlin and S. F Graebe. Issues in nonlinear stochastic grey-box identification. *International Journal of Adaptive Control and Signal Processing*, 9:465–490, 1995.

[3] P. D. Christofides, A. Armaou, Y. Lou, and A. Varshney. *Control and Optimization of Multiscale Process Systems*. Birkhäuser, Boston, 2008.

[4] R. Cuerno, H. A. Makse, S. Tomassone, S. T. Harrington, and H. E. Stanley. Stochastic model for surface erosion via ion sputtering: Dynamical evolution from ripple morphology to rough morphology. *Physical Review Letters*, 75:4464–4467, 1995.

[5] S. F. Edwards and D. R. Wilkinson. The surface statistics of a granular aggregate. *Proceedings of the Royal Society of London Series A - Mathematical Physical and Engineering Sciences*, 381:17–31, 1982.

[6] K. A. Fichthorn and W. H. Weinberg. Theoretical foundations of dynamical Monte Carlo simulations. *Journal of Chemical Physics*, 95:1090–1096, 1991.

[7] D. T. Gillespie. A general method for numerically simulating the stochastic time evolution of coupled chemical reactions. *Journal of Computational Physics*, 22:403–434, 1976.

[8] G. Hu, Y. Lou, and P. D. Christofides. Model parameter estimation and feedback control of surface roughness in a sputtering process. *Chemical Engineering Science*, 63:1810–1816, 2008.

[9] G. Hu, G. Orkoulas, and P. D. Christofides. Modeling and control of film porosity in thin film deposition. *Chemical Engineering Science,* accepted, 2009.

[10] S. Keršulis and V. Mitin. Monte carlo simulation of growth and recovery of silicon. *Matetial Science & Engineering B*, 29:34–37, 1995.

[11] N. R. Kristensen, H. Madsen, and S. B. Jorgensen. Parameter estimation in stochastic grey-box models. *Automatica*, 40:225–237, 2004.

[12] S. W. Levine and P. Clancy. A simple model for the growth of polycrystalline Si using the kinetic Monte Carlo simulation. *Modelling and Simulation in Materials Science and Engineering*, 8:751–762, 2000.

[13] Y. Lou and P. D. Christofides. Estimation and control of surface roughness in thin film growth using kinetic Monte-Carlo models. *Chemical Engineering Science*, 58:3115–3129, 2003.

[14] Y. Lou and P. D. Christofides. Feedback control of growth rate and surface roughness in thin film growth. *AIChE Journal*, 49:2099–2113, 2003.

[15] Y. Lou and P. D. Christofides. Feedback control of surface roughness using stochastic PDEs. *AIChE Journal*, 51:345–352, 2005.

[16] Y. Lou and P. D. Christofides. Nonlinear feedback control of surface roughness using a stochastic PDE: Design and application to a sputtering process. *Industrial & Engineering Chemistry Research*, 45:7177–7189, 2008.

[17] Y. Lou, G. Hu, and P. D. Christofides. Model predictive control of nonlinear stochastic partial differential equations with application to a sputtering process. *AIChE Journal*, 54:2065–2081, 2008.

[18] P. B. Maksym. Fast Monte Carlo simulation of MBE growth. *Semiconductor Science and Technology*, 3:594–596, 1988.

[19] D. Ni and P. D. Christofides. Multivariable predictive control of thin film deposition using a stochastic PDE model. *Industrial & Engineering Chemistry Research*, 44:2416–2427, 2005.

[20] J. S. Reese, S. Raimondeau, and D. G. Vlachos. Monte Carlo algorithms for complex surface reaction mechanisms: Efficiency and accuracy. *Journal of Computational Physics*, 173:302–321, 2001.

[21] T. Shitara, D. D. Vvedensky, M. R. Wilby, J. Zhang, J. H. Neave, and B. A. Joyce. Step-density variations and reflection high-energy electron-diffraction intensity oscillations during epitaxial growth on vicinal GaAs(001). *Physical Review B*, 46:6815–6824, 1992.

[22] D. G. Vlachos, L. D. Schmidt, and R. Aris. Kinetics of faceting of crystals in growth, etching, and equilibrium. *Physical Review B*, 47:4896–4909, 1993.

[23] D. D. Vvedensky, A. Zangwill, C. N. Luse, and M. R. Wilby. Stochastic equations of motion for epitaxial growth. *Physical Review E*, 48:852–862, 1993.

[24] L. Wang and P. Clancy. A kinetic Monte Carlo study of the growth of Si on Si(100) at varying angles of incident deposition. *Surface Science*, 401:112–123, 1998.

[25] L. Wang and P. Clancy. Kinetic Monte Carlo simulation of the growth of polycrystalline Cu films. *Surface Science*, 473:25–38, 2001.

[26] P. Zhang, X. Zheng, S. Wu, J. Liu, and D. He. Kinetic Monte Carlo simulation of cu thin film growth. *Vacuum*, 72:405–410, 2004.